A peer-reviewed version of this preprint was published in PeerJ on 28 July 2021.

View the peer-reviewed version (peerj.com/articles/11840), which is the preferred citable publication unless you specifically need to cite this preprint.

Tovar RU, Cantu V, Fremaux B, Gonzalez Jr P, Spikes A, García DM. 2021. Comparative development and ocular histology between epigean and subterranean salamanders (*Eurycea*) from central Texas. PeerJ 9:e11840 https://doi.org/10.7717/peerj.11840

Divergent patterns of ocular development and gene expression in the evolution of a subterranean salamander

Ruben U. Tovar Corresp., [1, 2] , **Valentin Cantu** [3, 4] , **Brian P. Fremaux** [1] , **Pedro Gonzalez** [1] , **Dana M. García** [1]

[1] Department of Biology, Texas State University, San Marcos, Texas, United States

[2] Department of Integrative Biology, University of Texas at Austin, Austin, TX, United States

[3] San Marcos Aquatic Resources Center, U.S. Fish and Wildlife Service, San Marcos, Texas, United States

[4] Uvalde National Fish Hatchery, U.S. Fish and Wildlife Service, Uvalde, TX, United States

Corresponding Author: Ruben U. Tovar
Email address: rubenut@utexas.edu

Relatively few studies have focused on the evolution and development of divergent nervous systems. The salamander clade (*Eurycea*) from the karst regions of central Texas provide an ideal platform for comparing divergent nervous and sensory systems, since some species exhibit extreme phenotypes thought to be associated with inhabiting a subterranean environment, including highly reduced eyes. We describe ocular development and examine early ocular protein expression (Pax6 and Shh), comparing between two salamander species representing two phenotypes: the surface dwelling Barton Springs salamander (*E. sosorum*) and the obligate subterranean Texas blind salamander (*E. rathbuni*). Between the two species, similarities during the development of ocular tissue (e.g. optic cup and lens vesicle) were observed during embryogenesis. However, during late stage embryogenesis the two species display markedly different patterns of Pax6 localization, which parallel patterns previously reported in a cavefish. A lens vesicle was observed in *E. rathbuni*embryos at stage 40, yet the lens is absent in adults, suggesting the regression of the lens during ontogeny. We also include adult histology of the surface dwelling San Marcos salamander (*E. nana*) and note similarities to *E. sosorum*. Adult *E. rathbuni*lack major histological features associated with vision; however, eye morphology did not differ significantly between *E. rathbuni*and *E. sosorum*in early developmental stages, suggesting a combination of underdevelopment and degeneration contribute to the reduced eyes of adult *E. rathbuni*.

Divergent patterns of ocular development and gene expression in the evolution of a subterranean salamander

Ruben U. Tovar[1,4], Valentin Cantu[2,3], Brian P. Fremaux[1], Pedro Gonzalez Jr.[1], Dana M. García[1]

[1]Department of Biology, Texas State University, San Marcos, Texas, 78666, USA.
[2]San Marcos Aquatic Resources Center, San Marcos, Texas, 78666, USA.
[3]Uvalde National Fish Hatchery, Uvalde, Texas, 78801, USA.
[4]Department of Integrative Biology, University of Texas at Austin, Austin, TX 78712 USA.

Corresponding Author:
Ruben U. Tovar
2415 Speedway, Austin, TX, 78712, USA
Email address: rubenut@utexas.edu

Abstract

Background. Relatively few studies have focused on the evolution and development of divergent nervous systems. The salamander clade (*Eurycea*) from the karst regions of central Texas provides an ideal platform for comparing divergent nervous and sensory systems since some species exhibit extreme phenotypes thought to be associated with inhabiting a subterranean environment, including highly reduced eyes.

Methods. We describe ocular development and examine early ocular protein expression (Pax6 and Shh), comparing between two salamander species representing two phenotypes: the surface dwelling Barton Springs salamander (*E. sosorum*) and the obligate subterranean Texas blind salamander (*E. rathbuni*).

Results. Between the two species, similarities in the development of ocular tissue (e.g. optic cup and lens vesicle) were observed during embryogenesis. However, during late stage embryogenesis the two species display markedly different patterns of Pax6 localization, which parallel patterns previously reported in a cavefish. A lens vesicle was observed in *E. rathbuni* embryos at stage 40, yet the lens is absent in adults, suggesting the regression of the lens during ontogeny. We also include adult histology of the surface-dwelling San Marcos salamander (*E. nana*) and note similarities to *E. sosorum*. Adult *E. rathbuni* lack major histological features associated with vision; however, eye morphology did not differ significantly between *E. rathbuni* and *E. sosorum* in early developmental stages, suggesting a combination of underdevelopment and degeneration contribute to the reduced eyes of adult *E. rathbuni*.

Introduction

Until the emergence of evolutionary developmental biology, studies aiming to understand the diversity of phenotypes observed in closely related species have been nested in either

morphological or genetic approaches. We sought to use both molecular and morphological approaches to compare evolutionary and developmental divergence between two karst salamander species which occupy different microhabitats.

Obligate aquatic subterranean fauna are referred to as stygobites (Goricki et al. 2012). Stygobitic morphology includes drastically reduced eyes and pale skin. This morphology is exemplified by the Texas blind salamander (*Eurycea rathbuni*) with its reduced pigment and eye structure (Mitchell and Redell, 1965). In contrast, the San Marcos salamander (*E. nana*) and Barton Springs salamander (*E. sosorum*) are surface species and have pigmented skin and seemingly well-developed eyes. Interestingly, there have been a number of subterranean invasions by the central Texas *Eurycea*, and phylogenetic analyses show strong support for a close relationship between the species with divergent ocular phenotypes (Bendick et al. 2013; Chippindale et al. 2000; Wiens et al. 2003). Ocular histology has been investigated in several families of salamanders (Fite, 1976; Linke et al. 1876; Roth, 1987), and differing degrees of ocular regression are documented in the subterranean species of the genera *Eurycea* (Eigenmann, 1900; Emerson, 1905), *Typhlotriton* (Walls, 1942), and *Proteus* (Möller, 1951). Ocular histology has been examined in *E. rathbuni* (Eigenmann, 1900), but no direct comparisons to surface relatives have been made, nor have the developmental processes leading to divergence been examined.

Herein, we present the ocular histology of three species of central Texas *Eurycea,* representing two phenotypes: the subterranean *E. rathbuni*, and the surface-dwelling *E. nana* and *E. sosorum*. We also use immunohistochemistry to compare expression of Paired box protein-6 (Pax6) and Sonic hedgehog protein (Shh), which are known to drive the development of the anterior-posterior axis of vertebrates, the central nervous system, and which have been observed

in cavefish ocular development (Jeffery, 2009). Moreover, this study investigates differences in eye tissue development that leads to patterns observed between surface and subterranean eyes. We also test the shifts in expression patterns of *pax6* and *shh* during development, shifts that contribute to ocular divergence observed within central Texas *Eurycea*.

Materials & Methods

Specimens.

The San Marcos Aquatic Resource Center (SMARC), Texas, United States Fish and Wildlife Service (USFWS) donated freshly dead adult specimens of Texas blind salamanders (*Eurycea rathbuni*; n = 3), San Marcos salamanders (*E. nana*; n = 3), and Barton Springs salamanders (*E. sosorum*; n = 3) to Texas State University in San Marcos, Texas. The specimens' heads were removed and transported to Texas State University for further processing under scientific permit number SPR-0390-045. General measurements along with tissue samples were taken from the remaining body which was then preserved in 95% ethanol and cataloged at the SMARC. Early stage embryos of *E. rathbuni* and *E. sosorum* were obtained from captive production at SMARC.

Fixation and Imaging.

Techniques for fixation of heads and embryos followed Neve et al. (2011) as described below. Tissues were placed in 4% buffered paraformaldehyde for 24 hours and washed three times for 10 minutes with phosphate buffered saline (PBS). Following fixation, tissues were placed in a 30% sucrose solution prepared in PBS for cryoprotection and stored at 4° C for at least 24 hours. Sections of adult tissue at 20 µm, and embryo tissue at 10 µm were collected using a Shandon Cryotome at -28° C, mounted on a slide using 90% glycerol, and stored at -20° C (Saul et al. 2010). At the conclusion of the

study sections were deposited at The University of Texas at Austin's Biodiversity Center. Images were acquired using an Olympus FV1000 equipped with differential interference contrast optics and a 10X objective.

Retinal and Ocular Measurements.

Images of ocular cross sections were opened in ImageJ software, and the measurement tool was calibrated to each image. One image from each individual representing the three species (*E. rathbuni,* N = 3; *E. nana,* N = 3; and *E. sosorum,* N= 3) was selected for measurement based on the presence of a lens (for *E. nana* and *E. sosorum*) in the section and the presence of six, clearly distinguishable retinal layers: photoreceptor/retinal pigment epithelial layer, outer nuclear layer (ONL), outer plexiform layer (OPL), inner nuclear layer (INL), inner plexiform layer (IPL) and retinal ganglion cell layer (RGL; see Fig. 2). Measurements of retinal width were obtained from a region where the OPL appeared undistorted, signifying that the section in that region was not oblique. Three measurements were taken per individual with the transect being orthogonal to the OPL. Three measurements for each retinal layer were also obtained from each individual in the region of the transect. The means of the triplicate measurements were used to provide an estimate of thicknesses for that individual, and the three individuals provided an estimate of population means for their respective species (N = 3). Thirty-four adult and three early developmental stage specimens of *E. sosorum* and *E. rathbuni* were obtained from SMARC and imaged using a Nikon D7000. Eye and head length measurements were obtained using ImageJ. Both eye and head measurements of each species were tested for normality. An analysis of variance (ANOVA) was conducted using eye measurements taken from adults and earlier developmental stages (standardized by head length) for each of the two species.

Immunohistochemistry and Imaging.

Immunohistochemistry using transverse sections of embryo eyes was accomplished by blocking with 3% bovine serum albumin dissolved in PBS (Sigma Aldrich, A7030-10G) for two hours, then washing three times for ten minutes with PBS with (0.05% Tween). Each primary and secondary antibody was diluted as shown in Table 2. Sections were incubated with primary antibody for two hours at room temperature and with secondary antibody for two hours at room temperature. Two fifteen-minute washes were implemented between each incubation period using PBS. Finally, the nuclear stain Hoechst was applied for twenty minutes, after which sections were given two fifteen-minute washes with PBS. Coverslips were mounted in 90% glycerol, and slides were stored at 4°C until imaged. Images were obtained using an Olympus FV-1000 scanning confocal microscope. Confocal settings for each of the three fluors were initially optimized on an *E. sosorum* sample, and settings remained constant while acquiring each successive image.

Results

Adult Ocular Histology and Measurements from *Early Stage and Adult Eyes*

Examination of adult ocular sections taken from two surface species and a subterranean species reveal markedly different histology between the two phenotypes. Histological sections from the surface species *Eurycea nana* and *E. sosorum* revealed well-defined retinal layers, corneal layers, iris, lens, and pigment epithelium (Fig. 1 and 2). Retinal layers were identified as retinal pigment epithelium (RPE), photoreceptors (PR), outer nuclear layer (ONL), outer plexiform layer (OPL), inner nuclear layer (INL), inner plexiform layer (IPL), and retinal ganglion layer (RGL). Although a nerve fiber layer was not always apparent (see Figure 1D for an exception), a well-defined optic nerve was observed in both species. In the surface salamanders, melanized tissue is restricted primarily to the PE, the choroid, the ciliary body of

the iris; however, some dark pigmentation was also observed outside the sclera and surrounding the optic nerve.

Features previously described by Eigenmann (1900) for *Eurycea rathbuni* were identified and included optic nerve (ON), ganglion layer (GL), outer and inner reticular layer (O/IRL), and pigment epithelium (PE). No lens was identified. A well-defined optic nerve was observed emanating from the eyes of *E. rathbuni* (Fig. 3). The entire ocular structure is surrounded by melanized tissue.

There were no significant differences ($P > 0.05$) in the overall thickness of the retina or the thickness of component layers when comparisons were made between sections taken from *E. sosorum* and *E. nana* (Table 1). The thickest layer of the retina in both species is the inner nuclear layer (INL), which contains the cellular nuclei of bipolar cells, horizontal cells and amacrine cells, and represents 22.9% of the retinal thickness in *E. nana* and 26.0% in *E. sosorum* (Table 1).

In order to explicitly test whether the eye of *E. rathbuni* adults were underdeveloped compared to *E. sosorum*, measurements of the whole eye scaled to head length were obtained from animals early in development (stages 37 and 40) for *Eurycea rathbuni* (n=3) and *E. sosorum* (n=3), and from adult *E. rathbuni* (n=34) and *E. sosorum* (n=36) *E. nana* individuals were not included in this analysis as we did not have early developmental stages for this *species*. A one-way ANOVA and a post-hoc Tukey's HSD test (Table 3) revealed a difference between adult *E. sosorum* and all other groups (Tukey's HSD $P<0.001$). There were no differences in the size of the eye between adult *E. rathbuni* and either species in their early developmental stages (Table 3).

Pax6 and Shh Localization

Due to the limited availability of embryos, only stages 37 and 40 following staging by Duellman and Trueb (1994), are presented in this study. Pax6 and Shh proteins are observed in the two phenotypes represented by *E. rathbuni* (subterranean phenotype) and *E. sosorum* (surface phenotype). During development in both species Shh is expressed in select cells surrounding the midbrain and optic cup of (Fig.4). The expression of Pax6 is also observed in and around the midbrain, optic cup, and lens vesicle of both species. The expression of Pax6 in stage 40 of *E. rathbuni* is noticeably reduced compared to stage 37 in the same species, and to both developmental stages of *E. sosorum*. Pax6 is strongly expressed in the tissue surrounding the developing optic cup of *E. sosorum* and in the lens with particularly noticeable expression within the lens of at stage 40.

Discussion

Adult Ocular Histology

This study provides a foundation of descriptive ocular histology comparing three closely related species and two ecotypes, surface and subterranean. *Eurycea rathbuni* has drastically reduced eyes, a characteristic widely accepted as reflecting adaptation to subterranean life and exemplified by other stygobitic organisms, including other cave dwelling salamanders (e.g., *Proteus anguius*), cave-dwelling fish (e.g., *Astyanax mexicanus*), as well as extremely phylogenetically divergent invertebrates (Romero, 2009). *Eurycea rathbuni* exhibits a few vestigial retinal layers surrounded by melanized tissue. These results suggest light - were it available - would be unable to pass through the pigment epithelium to be utilized by photoreceptors if there were any. Nevertheless, the optic nerve is still present in *E. rathbuni*, suggesting possible sensory function, but probably not vision (Fig. 3).

Upon close examination of *E. rathbuni* histology, the feature identified by Eigenmann (1900) as an optic nerve penetrating to the center of the eye resembles the hyaloid canal. The hyaloid canal provides vascularization to the developing lens during early embryogenesis (Dunlop et al. 1997). Early hyaloid vascularization occurs when the hyaloid artery and vein follow the optic fissure via the optic stalk distally, eventually reaching the optic cup and lens vesicle, where they provide the necessary vascularization for the continued development of the lens. We found that ocular development in *E. rathbuni* progresses to the point of a lens vesicle (Fig. 4); therefore, it is likely that hyaloid vascularization is present during development.

The surface species *E. nana* and *E. sosorum* have well developed retinal layers, including photoreceptors and pigment epithelium, exhibiting ocular anatomy expected of surface species (Linke et al. 1876; Heatwole, 1998). The surface species also exhibit a lens, cornea, iris, and have a well-developed optic nerve. Taken together, it appears that all the ocular structures necessary to support vision are in place. The measurements between *E. nana* and *E. sosorum* of the INL and photoreceptor layer (PRL) relative to the entire retina (Table 1), suggests a morphological difference not yet fully understood. One possibility may be differences consequent to adaptions to either diurnal or nocturnal lifestyles, differing degrees of subterranean life histories, or the potential hybridization with other species, for example, *E. neotenes* with the stygobitic species *E. tridentifera* (Sweet, 1984). When total retinal measurements were analyzed between the two phenotypes using a mixed effect model, no difference was observed. We speculate that while the retina of *E. rathbuni* is under-differentiated, it accounts a greater volume of the reduced eye and appears as not being significantly different from its surface relatives. When eye length was measured between early development and adult between the two species, no differences were observed between adult *E. rathbuni* and either of the species in early

development (Fig. 5). This result suggests that underdevelopment, i.e. a failure of development to progress, may underlie the reduced eye size in *E. rathbuni*.

Fundamental knowledge of ocular anatomy has important implications for current research involving the central Texas *Eurycea*. For example, the full extent of visual function in the surface species may have implications regarding mate choice and predator or prey recognition. Future quantification of photoreceptors and their associated wavelength optima could elucidate the extent of color perception and the preferred active time during the day (e.g. nocturnal, diurnal, or crepuscular).

Pax6 and Shh Localization

Compared spatially, the localization of Pax6 and Shh proteins through development of *E. rathbuni* and *E. sosorum* is similar and follow what is expected during vertebrate neurulation. Specifically, the genes are expressed in the developing central nervous system, including the brain and eye (Gilbert, 2010). The continued expression of *pax6* and *vax1* genes is important as they encode transcription factors that bind with the enhancer sequence of the *δ-crystallin* gene, which in turn encodes the crystalline proteins found in the lens (Gilbert, 2010). If *pax6* gene expression is down regulated during the development of the lens, the lens will cease to develop. In the subterranean fish *Asytanax mexicanus*, the down regulation of *pax6* gene consequent to upregulation of *shh* expression contributes to apoptosis of the lens, which stunts further retinal differentiation and results in the formation of vestigial remnants of retina found in cave-dwelling *A. mexicanus* (Jeffery, 2005).

The histology of adult *Eurycea sosorum* reflects a well-organized, functional eye, suggesting the continued availability of Pax6 protein well into the late stages of development. In the newt *Cynops pyrrhogaster*, *pax6* gene expression persists through adulthood and plays an

important role in regeneration when the animal is subjected to retinal injury (Del Rio-Tsonis et al. 1995). The expression of the *pax6* gene in *E. sosorum* follows the canonical developmental expression of a vertebrate with vision. The labeling of the Shh protein is also observed in *E. sosorum*, as expected in vertebrate development, and it does not appear to be highly expressed.

In *E. rathbuni* the presence of Pax6 protein is noted early in development at stage 37 and is spatially distributed in the developing brain and eye in a pattern similar to that seen in *E. sosorum*. However, Pax6 is undetectable at stage 40, suggesting little expression in *E. rathbuni*. During these late stages Shh continues to be expressed. Shh-labeling at stages 37 and 40 is observed in select cells with high levels relative to adjacent cells; some of the *shh*-expressing cells are in close proximity to the developing eye (Fig. 4). The continued expression of *shh* during late stage development in *E. rathbuni,* particularly its concentration in specific cells surrounding the eye and forebrain, plus the reduced expression of Pax6, is consistent with down regulation of the Pax6 caused by Shh. This pattern is reminiscent of the expression pattern observed in cavefish (Jeffery, 2009). Similar patterns of ocular development also occur, particularly in the development of a lens in the subterranean *E. rathbuni*. Together, both the development of a lens and the localization patterns of Pax6 and Shh suggest a degree of convergent evolution with *A. mexicanus*.

The expression of *pax6* and *shh* suggests their potential for driving differences in ocular development. Observing Pax6 and Shh proteins in later stages of *E. sosorum* and *E. rathbuni* is needed to understand the completion of retinal development in *E. sosorum* and lens degeneration in *E. rathbuni*. Moreover, later stages would allow understanding of the molecular underpinnings in lens degeneration, and specifically address the potential of apoptosis as a means to eye regression as seen in *A. mexicanus*. Importantly, the overall ontogeny and expression of Pax6

239 and Shh proteins during ocular development of the two salamander phenotypes parallel the two
240 phenotypes explored in the *A. mexicanus* (Jeffery, 2009). This parallel suggests that the
241 salamanders examined in this study and the teleost fish examined by Jeffery (2009) may share a
242 degree of convergent evolution in development and in the molecular mechanisms (*pax6* and *shh*)
243 responsible for the divergent ocular phenotypes in two vertebrate lineages occupying similar
244 subterranean habitats. Studies incorporating intermediate stages are needed to determine the
245 divergence of tissue and gene expression between the two phenotypes, and if, as reported by
246 Jeffery et al. (2009), these early expression patterns lead to apoptosis of the lens.

247 ## Conclusions

248 The comparative examination of ocular histology suggests *E. nana* and *E. sosorum* are
249 capable of phototransduction while development of the retina in *E. rathbuni* is aborted during
250 development, and the lens is lost at some point during ontogeny. We observed similar ocular
251 development between the two phenotypes, including the development of a lens in *E. rathbuni*.
252 Taken together, parallels during early embryonic development were observed between the two
253 phenotypes, whilst ocular morphology and histology in adults is drastically different.
254 Furthermore, these results raise interesting questions about the evolution of subterranean
255 phenotypes and the selective pressures they experience, or in the case of the eye, how they are
256 lost and what implications this might have with respect to the molecular mechanisms responsible
257 for their development.

258 This study provides a platform using a stygobitic tetrapod to understand the evolutionary
259 developmental biology of eye reduction. Moreover, a non-transgenic tetrapod model may
260 provide novel insight to the genes and their regulation in developing a healthy eye. In the future,
261 we hope to use multiple species from this clade and sequencing approaches incorporating

intermediate stages to better understand the evolution and underlying genetic mechanisms responsible for the diverse subterranean phenotypes.

Acknowledgements

We thank the U.S. Fish and Wildlife Service Aquatic Recourse Center San Marcos, TX, for the continued support of this research including access to facilities and captive populations of salamanders. We also thank Drs. Nihal and Sunethra Dharmasiri for generously allowing us to image using their stereomicroscope. The confocal microscope was purchased with an NSF MRI grant DBI-0821252 at Texas State University.

References

1. Bendick, Nathan F., Jesse M. Meik, Andrew G. Gluesenkamp, Corey E. Roelke, and Paul T. Chippindale. (2013) Biogeography, phylogeny, and morphological evolution of central Texas cave and spring salamanders. *Evolutionary Biology*.13: 201.

2. Chippindale, Paul T., Andrew H. Price, John J. Wiens, and David M. Hillis. (2000) *Herpetological Monographs: Phylogenetic Relationships and Systematic Revision of Central Texas Hemidactyliine Plethodontid Salamanders*. 14. Emporia: The Herpetologists' League. 1-80.
3. Duellman, William E., and Linda Trueb. (1994) *Biology of Amphibians*. Baltimore: The Johns Hopkins University Press, 1994. 109-132.
4. Dunlop, S.A., S.R. Moore, and L.D. Beazley. (1997) Changing Patterns of Vasculature in the Developing Amphibian Retina. The Journal of Experimental Biology. 200: 2479-2492.
5. Eigenmann, Carl H. (1900) The Eyes of the Blind Vertebrates of North America, II. The Eyes of *Typhomolge rathbuni* Stejneger. *Transactions of the American Microscopical Society.* 21: 49-56, 58-60.
6. Emerson, Ellen T. (1905) General Anatomy of *Typhlomolge rathbuni*. *Proceedings of the Boston Society of Natural History*. 32: 43-75.
7. Fite, KatherineV. (1976) *The amphibian visual system. A multidisciplinary approach*. Academic Press, London New York. 225-305.
8. Goricki, Spela, Niemiller, Mathew L. Fenolio, Dante B. (2012) *Salamanders, Encyclopedia of Caves*. Ed. White, William B., Culver, David C. Massachusetts: Academic Press, Elsevier. 665-676.
9. Heatwole, Harold. (1998) *Amphibian Biology Volume 3, Sensory Perception*. Chipping Norton: Surrey Beatty and Sons. 797-807.
10. Jeffery, William R. (2005) Adaptive Evolution of Eye Degeneration in the Mexican Blind Cavefish. *Journal of Heredity*.96(3): 185-196.
11. Jeffery, William R. (2009) Evolution and Development in the Cavefish Astyanax. *Evolution and Development*. 86:191-221.
12. Linke R, Roth G, Rottluff B. (1876) Comparative studies on the eye morphology of lungless salamanders, family Plethodontidae, and the effect of miniaturization. *Journal of Morphology*.189: 131-143.
13. Mitchell, R. W. and J. R. Reddell. (1965) *Eurycea tridentifera* a new species of troglobitic salamander from Texas and a reclassification of *Typhlomolge rathbuni*. *Texas Journal of Science*.17: 12-20.

14. Möller A. (1951) Die Struktur des Auges bei Urodelen verschiedener KorpergroBe. Zool. *Jahrb. Physiol*. 62: 138-182.

15. Romero, Aldemaro. (2009) *Cave Biology Life in Darkness*. New York: Cambridge University Press.130-158.

16. Roth, Gerhard. (1987) *Visual Behavior in Salamanders*. Germany. Springer-Verlag Berlin Heidelberg. 89-128.

17. Saul, Katherine E., Joseph R. Koke and Dana M. García. (2010) Activating ranscription factor 3 (ATF3) expression in the neural retina and optic nerve of zebrafish during optic nerve regeneration. *Comparative Biochemistry and Physiology, part A*, 155: 172-182.

18. Schneider, C.A., Rasband, W.S., Eliceiri, K.W. (2012) NIH Image to ImageJ: 25 Years of Image Analysis. *Nature Methods*. 9: 671-675.

19. Sweet, S. Samuel. (1984) Secondary Contact and Hybridization in the Texas Cave Salamanders *Eurycea neotenes* and *E. tridentifera*. Copeia: 2: 428-441.

20. Wiens, John J., Paul T. Chippindale, David M. Hillis. (2003) When Are Phylogenetic Analyses Misled by Convergence? A Case Study in Texas Cave Salamanders. *Systematic Biology: A Journal of the Society of Systematic Biologists*. 52.4: 501-514.

Figure 1(on next page)

Sections of adult E. nana (A, C and D) and E. sosorum (B) eye.

Illustrating regions of the posterior eye showing well-developed retinal layers and pigment (A, B, D). The lens, cornea, and iris are also visible (A, B, C). Images were acquired using an Olympus XLUMPlanFI 20x lens with a numerical aperture of 0.95, and optimized for contrast. No staining was used.

PeerJ Preprints | https://doi.org/10.7287/peerj.preprints.27301v1 | CC BY 4.0 Open Access | rec: 29 Oct 2018, publ: 29 Oct 2018

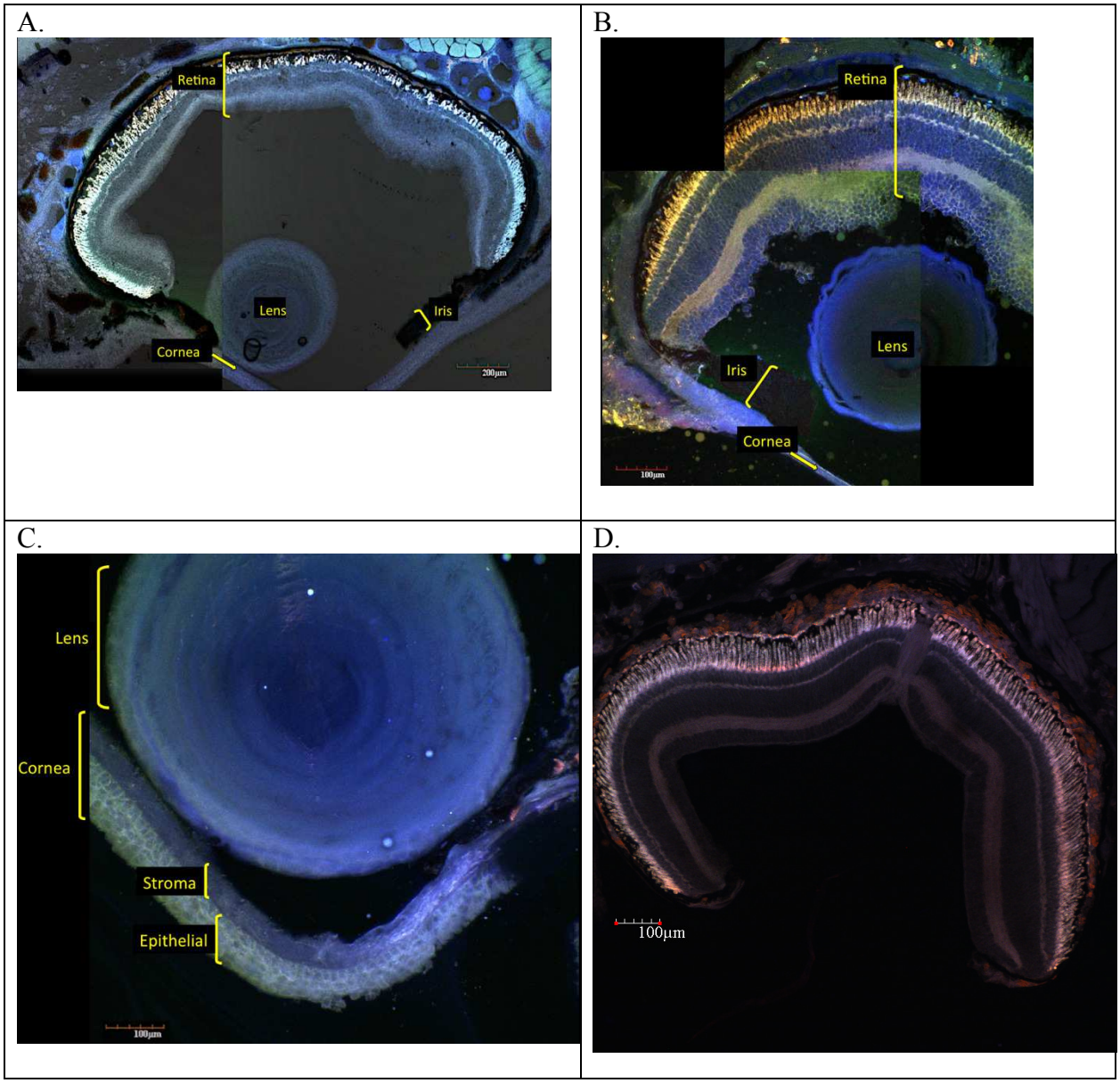

FIGURE 1. Sections of adult *E. nana* (A, C and D) and *E. sosorum* (B) eye. Illustrating regions of the posterior eye showing well-developed retinal layers and pigment (A, B, D). The lens, cornea, and iris are also visible (A, B, C). Images were acquired using an Olympus XLUMPlanFI 20x lens with a numerical aperture of 0.95, and optimized for contrast. No staining was used.

PeerJ Preprints | https://doi.org/10.7287/peerj.preprints.27301v1 | CC BY 4.0 Open Access | rec: 29 Oct 2018, publ: 29 Oct 2018

Figure 2(on next page)

Ocular sections of adult *E. nana*and *E. sosorum*.

Associated retinal layers (A), pigment epithelium (PE), photoreceptor layer (PR), outer nuclear layer (ONL), outer plexiform layer (OPL), inner nuclear layer (INL), inner plexiform layer (IPL), retinal ganglion cell layer (RGCL). Ocular sections of adult *E. sosorum*and associated retinal layers (B). Ocular section of adult *E. nana*exemplifying the optic nerve (C). Ocular section of adult *E. sosorum*showing the optic nerve (D). Images were acquired using an Olympus XLUMPlanFI 20x lens with a numerical aperture of 0.95, and optimized for contrast. No staining was used.

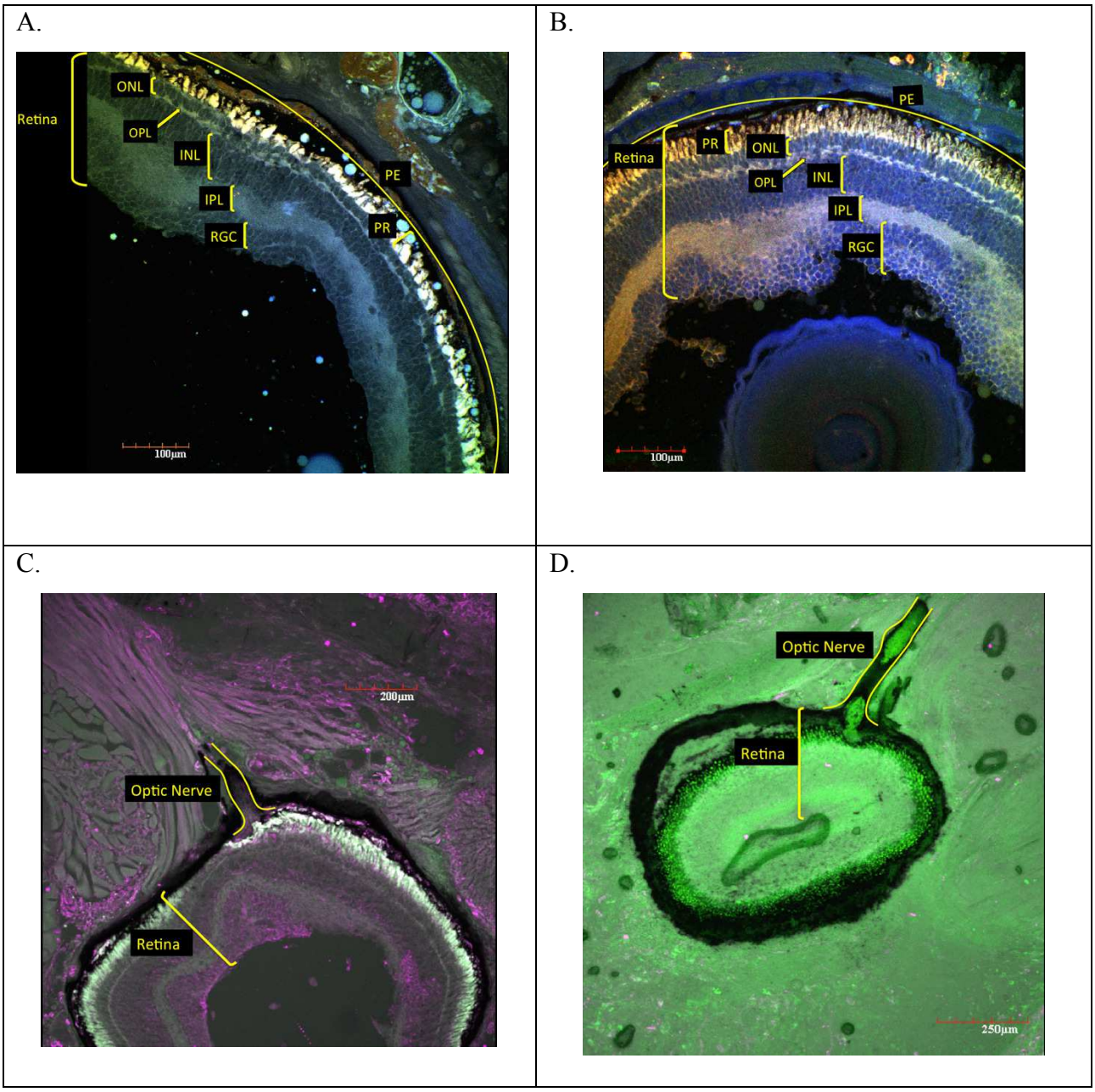

FIGURE 2. Ocular sections of adult *E. nana* and *E. sosorum*. Associated retinal layers (A), pigment epithelium (PE), photoreceptor layer (PR), outer nuclear layer (ONL), outer plexiform layer (OPL), inner nuclear layer (INL), inner plexiform layer (IPL), retinal ganglion cell layer (RGCL). Ocular sections of adult *E. sosorum* and associated retinal layers (B). Ocular section of adult *E. nana* exemplifying the optic nerve (C). Ocular section of adult *E. sosorum* showing the optic nerve (D). Images were acquired using an Olympus XLUMPlanFI 20x lens with a numerical aperture of 0.95, and optimized for contrast. No staining was used.

PeerJ Preprints | https://doi.org/10.7287/peerj.preprints.27301v1 | CC BY 4.0 Open Access | rec: 29 Oct 2018, publ: 29 Oct 2018

Figure 3(on next page)

Adult *E. rathbuni*ocular sections.

Showing undifferentiated tissue layers surrounded by pigment epithelium (A). Identification of labels is as follows: optic nerve (ON), pigment epithelium (PE), ganglion layer (GL), inner reticular layer (IR), outer and inner reticular layer of the retina (O/I).Evidence of optic nerve also attached to the posterior region of the vestigial eye (A), and an optic nerve image taken at higher magnification and outlined in yellow (B). Images were acquired using an Olympus XLUMPlanFI 20x lens with a numerical aperture of 0.95, and optimized for contrast. No staining was used.

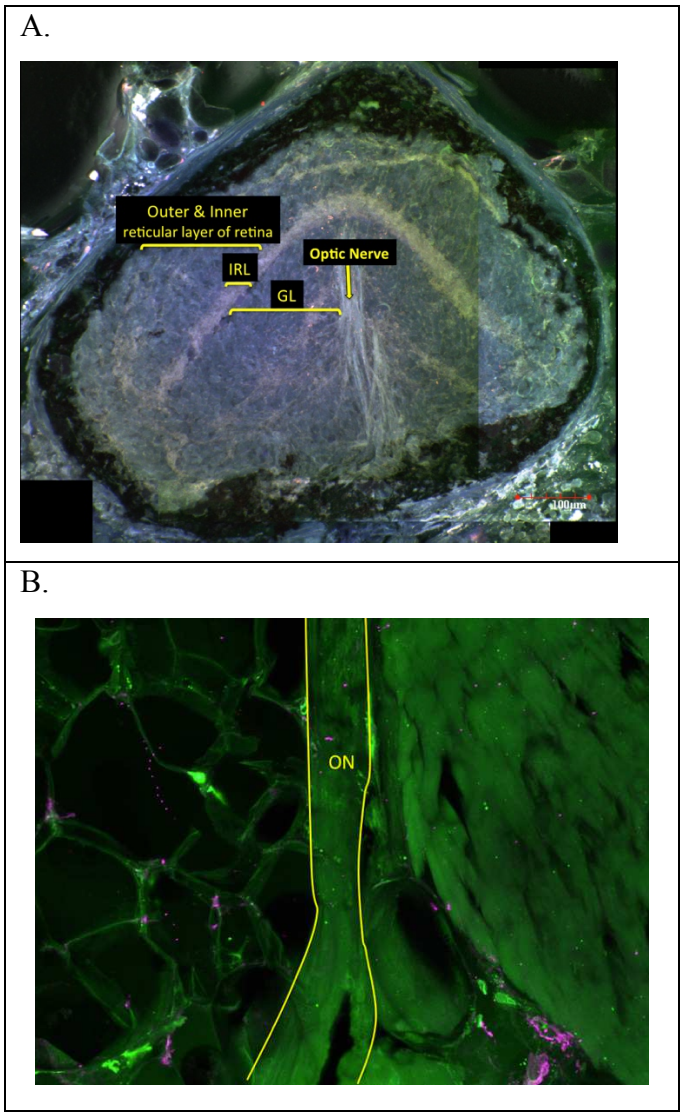

FIGURE 3. Adult *E. rathbuni* ocular sections. Showing undifferentiated tissue layers surrounded by pigment epithelium (A). Identification of labels is as follows: optic nerve (ON), pigment epithelium (PE), ganglion layer (GL), inner reticular layer (IR), outer and inner reticular layer of the retina (O/I). Evidence of optic nerve also attached to the posterior region of the vestigial eye (A), and an optic nerve image taken at higher magnification and outlined in yellow (B). Images were acquired using an Olympus XLUMPlanFI 20x lens with a numerical aperture of 0.95, and optimized for contrast. No staining was used.

Figure 4(on next page)

Two stages comparing *E. rathbuni*and *E. sosorum*ocular development with Pax6 and Shh labeling.

One stain and two antibodies were used to visualize protein labeling integral to ocular development, and included; Hoechst nuclear stain, *Shh*, *Pax6*. Respective days post oviposition (P.O.), and specimen images on the left. Arrows indicate lens development in the latter stages. Confocal images were acquired using an Olympus PlanApo 60x oil lens with a numerical aperture of 1.40.

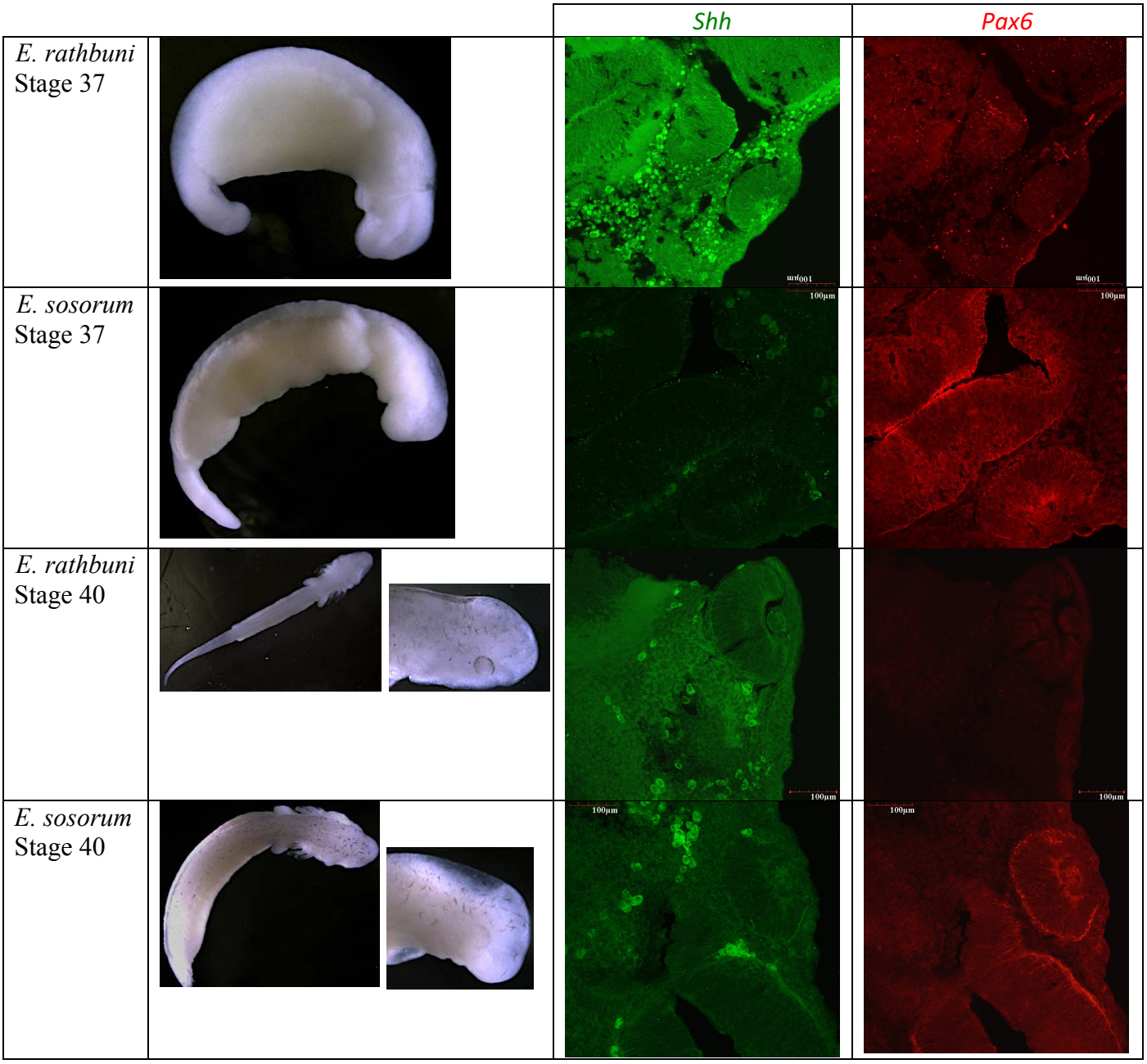

FIGURE 4. Two stages comparing *E. rathbuni* and *E. sosorum* ocular development with Pax6 and Shh labeling. One stain and two antibodies were used to visualize protein labeling integral to ocular development, and included; Hoechst nuclear stain, *Shh*, *Pax6*. Respective days post oviposition (P.O.), and specimen images on the left. Arrows indicate lens development in the latter stages. Confocal images were acquired using an Olympus PlanApo 60x oil lens with a numerical aperture of 1.40.

Figure 5(on next page)

Eye sizes for two species of salamander at different stages of development.

Two developmental stages (early vs. adult) were measured for two species from the central Texas *Eurycea*clade exemplifying subterranean (*E. rathbuni*) and surface (*E. sosorum*) optics. ANOVA and a post-hoc Tukey's test revealed that the ocular length of the adult *E. sosorum* was statistically significantly larger than the early stage *E. sosorum*and early and adult *E. rathbuni*. In contrast, there was no statistically significant difference between the ocular length of adult *E. rathbuni*and either embryonic salamander.

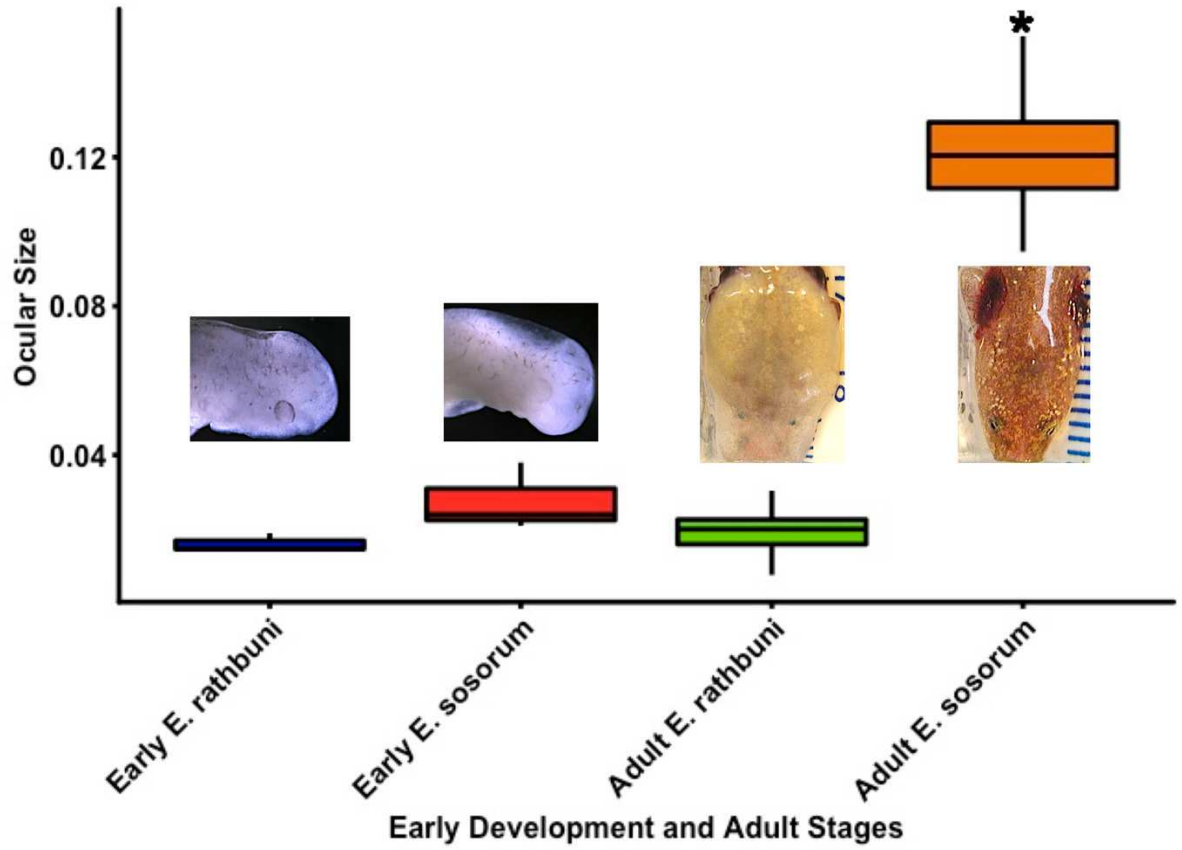

Fig. 5. Eye sizes for two species of salamander at different stages of development. Two developmental stages (early vs. adult) were measured for two species from the central Texas *Eurycea* clade exemplifying subterranean (*E. rathbuni*) and surface (*E. sosorum*) optics. ANOVA and a post-hoc Tukey's test revealed that the ocular length of the adult *E. sosorum* was statistically significantly larger than the early stage *E. sosorum* and early and adult *E. rathbuni*. In contrast, there was no statistically significant difference between the ocular length of adult *E. rathbuni* and either embryonic salamander.

Table 1 (on next page)

Thickness of the retina and its component layers.

[1]RGCL = retinal ganglion cell layer; IPL = inner plexiform layer; INL = inner nuclear layer; OPL = outer plexiform layer; ONL = outer nuclear layer; RPEPRL = combined retinal pigment epithelium and photoreceptor layers; RET = entire retina[2]N = 3 individuals for all data. [3]P-values were computed from a two-tailed, Student's T-test.

Table 1: Thickness of the retina and its component layers.

	Mean[2] Thickness ± SEM (μm)		
	E. sosorum	*E. nana*	P-value[3]
RGCL	50 ± 10	52 ± 3	0.9
IPL	34 ± 6	38 ± 5	0.7
INL	66 ± 5	69 ± 6	0.8
OPL	9.9 ± 0.9	9 ± 1	0.6
ONL	32 ± 3	29 ± 5	0.6
RPEPRL	49 ± 5	64 ± 4	0.08
RET	244 ± 7	260 ± 22	0.61

[1]RGCL = retinal ganglion cell layer; IPL = inner plexiform layer; INL = inner nuclear layer; OPL = outer plexiform layer; ONL = outer nuclear layer; RPEPRL = combined retinal pigment epithelium and photoreceptor layers; RET = entire retina

[2]N = 3 individuals for all data.

[3]P-values were computed from a two-tailed, Student's T-test.

Table 2(on next page)

Antibodies and respective concentrations.

Table 2. Antibodies and respective concentrations.

Antibody or Stain	Supplier/ Catalog number	Concentration or Dilution
Biotinylated anti-mouse, rat, chicken Pax6 antibody	R&D Systems Inc. #BAM1260	20 µg/mL
Streptavidin Cy-5	Invitrogen #43-8316	1:50
Anti-SHH, antibody produced in rabbit, affinity isolated antibody	Sigma-Aldrich #AV4423	1:100
Anti-rabbit IgG (FITC conjugated) antibody developed in goat	Sigma-Aldrich #F0382	1:80

Table 3(on next page)

One way ANOVA comparing eye size including early development and adult stages of *E. rathbuni*and *E. sosorum*.

Table 3. One way ANOVA comparing eye size including early development and adult stages of *E. rathbuni* and *E. sosorum*.

	Early *E. rathbuni*	Early *E. sosorum*	Adult *E. rathbuni*
Early *E. sosorum*	P>0.05	-	-
Adult *E. rathbuni*	P>0.05	P>0.05	-
Adult *E. sosorum*	**P<0.001	**P<0.001	**P<0.001